Bioorganic & Medicinal Chemistry 19 (2011) 4135–4143

Contents lists available at ScienceDirect

Bioorganic & Medicinal Chemistry

journal homepage: www.elsevier.com/locate/bmc

# Cell uptake of a biosensor detected by hyperpolarized $^{129}$Xe NMR: The transferrin case

Céline Boutin [a], Antoine Stopin [b], Fatimazohra Lenda [b], Thierry Brotin [b], Jean-Pierre Dutasta [b], Nadège Jamin [c], Alain Sanson [c], Yves Boulard [d], François Leteurtre [d], Gaspard Huber [a], Aurore Bogaert-Buchmann [a], Nawal Tassali [a], Hervé Desvaux [a], Marie Carrière [a], Patrick Berthault [a,*]

[a] CEA, IRAMIS, SIS2M, Laboratoire Structure et Dynamique par Résonance Magnétique, UMR CEA/CNRS 3299, 91191 Gif sur Yvette, France
[b] Laboratoire de Chimie de l'ENS Lyon, UMR 5182 CNRS-ENS Lyon, 46 Allée d'Italie, 69364 Lyon Cedex 07, France
[c] CEA, iBiTec-S, SB2SM, URA CEA/CNRS 2096, 91191 Gif sur Yvette, France
[d] CEA, iBiTec-S, SBIGeM, LBI, 91191 Gif sur Yvette, France

ARTICLE INFO

*Article history:*
Received 24 February 2011
Revised 26 April 2011
Accepted 1 May 2011
Available online 6 May 2011

*Keywords:*
Biosensors
Cryptophane
Xenon
Cells
NMR
Hyperpolarization

ABSTRACT

For detection of biological events in vitro, sensors using hyperpolarized $^{129}$Xe NMR can become a powerful tool, provided the approach can bridge the gap in sensitivity. Here we propose constructs based on the non-selective grafting of cryptophane precursors on holo-transferrin. This biological system was chosen because there are many receptors on the cell surface, and endocytosis further increases this density. The study of these biosensors with K562 cell suspensions via fluorescence microscopy and $^{129}$Xe NMR indicates a strong interaction, as well as interesting features such as the capacity of xenon to enter the cryptophane even when the biosensor is endocytosed, while keeping a high level of polarization. Despite a lack of specificity for transferrin receptors, undoubtedly due to the hydrophobic character of the cryptophane moiety that attracts the biosensor into the cell membrane, these biosensors allow the first in-cell probing of biological events using hyperpolarized xenon.



## 1. Introduction

There is a worldwide effort to propose hyperpolarized species for molecular imaging applications based on magnetic resonance. In this growing field, hyperpolarized xenon occupies a special and well-recognized position as a powerful magnetic resonance sensor of molecular or biological events. This is due to the huge signal obtained by the prior optical pumping[1] or dynamic nuclear polarization[2] step, to its exogenous and gaseous nature, and also to the wide chemical shift range spanned by this atom, which has a big deformable electron cloud.[3] Using these properties, an approach has been envisioned where the hyperpolarized noble gas is targeted to biological receptors via functionalized host systems.[4,5] When encapsulated in the core of transporters made by cage-molecules such as cryptophanes[6] or nanoparticles,[7] xenon has a specific resonance frequency which enables its discrimination from free xenon in spectroscopic imaging.[8]

Whereas the proof-of-concept of this approach has been successfully achieved in isotropic solution by several groups,[9–13] it has never been tested in vitro (or in vivo) by performing hyperpolarized $^{129}$Xe NMR experiments directly with cell suspensions. Recently Dmochowski's group proposed an original biosensor construction based on the functionalization of cryptophane with a cell-penetrating peptide.[14] Fluorescence tests on living cells were performed but no hyperpolarized $^{129}$Xe NMR experiment was presented. The experimental implementation appears demanding. Studying live cell suspensions by NMR requires a compromise regarding cell density, which must be high enough to reach a concentration compatible with the monitoring of cellular biological events, but not too high otherwise cell lifetime will be too short. Also a contrast mechanism, where the free and bound biosensor signals are discriminated, is needed to ensure that the biological event is really detected. For approaches using hyperpolarization, this means dealing with concentrations in the pico- to nanomolar range and managing more efficiently the nuclear spin relaxation induced by the presence of paramagnetic agents (ions, metalloproteins, dissolved oxygen, etc.).

Here the interaction of a biosensor of transferrin receptors (TfR) is detected via hyperpolarized $^{129}$Xe NMR of cell suspensions, and the NMR results are correlated with fluorescence microscopy. This system has been chosen for the following reasons: (i) it is a well-described system: transferrin (Tf), a naturally existing protein, has already received considerable attention in the area of drug targeting since it is biodegradable, non-toxic, and nonimmunogenic;[15] (ii) the biological targets are cell surface receptors and so

* Corresponding author. Tel.: +33 1 69 08 42 45; fax: +33 1 69 08 98 06.
*E-mail address:* patrick.berthault@cea.fr (P. Berthault).

0968-0896/$ - see front matter © 2011 Elsevier Ltd. All rights reserved.
doi:10.1016/j.bmc.2011.05.002

are easily reachable by dissolved xenon; (iii) these receptors can be abundant (up to 1.6 $10^5$ on the cell surface) for some cell lines;[16,17] (iv) endocytosis due to Tf–TfR complex formation is likely to further increase the local density of xenon receptors.

## 2. Results and discussion

### 2.1. Design and synthesis of the TfR sensors

It is known that the molecular systems for which xenon exhibits the highest affinity are cryptophanes, aromatic cage-molecules made of two cyclotriveratrylene bowls joined by aliphatic linkers. Consequently they constitute the core of our $^{129}$Xe NMR-based biosensors. A tether comprising a polyethylene spacer ended by an activated ester was first grafted on the cryptophane to produce precursor **1** (Fig. 1). The choice of four O–$CH_2$–$CH_2$ groups to constitute the spacer gave the cryptophane moiety flexibility, which was expected to be sufficient to avoid broad lines for encapsulated xenon caused by too fast transverse relaxation.[18] This spacer was also expected to be long enough to avoid multiplicity of the signals of encapsulated xenon when using the cryptophane racemic mixture.[19] The activated group of the cryptophane moiety was chosen to react with accessible primary amines, that is, ε-amine on lysine residues and α-amine groups at the N-termini of proteins. Cross-linking reagents such as *N*-hydroxysuccinimide esters are currently used to investigate protein–protein interactions,[20] but are characterized by a fast hydrolysis.[21] In order to minimize such deactivation phenomena by hydrolysis, a pentafluorophenol ester end[22] was used for the grafting step on the protein. Such a construction presents many advantages: (i) the same cryptophane-PEG-activated ester precursor can be used for the design of various biosensors, since it can be non-specifically grafted on any protein with lysine residues on its surface; (ii) if more than one lysine is present on the surface of the protein, several cryptophane cores can be grafted, therefore increasing the number of xenon binding sites and accordingly enhancing the intrinsic NMR sensitivity of the biosensor; (iii) provided that lysine residues are distant from the protein active site, due to the small size of cryptophane compared with that of the protein, it is expected that the affinity of the biosensor for the biological receptors is preserved.

Transferrin is a globular protein of molecular weight ~80,000 Dalton. It possesses 54 Lys residues, 23 of which are located on its external surface, and its holo form contains two iron atoms (Fig. 2a). The cryptophane precursor was grafted on the protein using the procedure detailed in Section 4. The affinity of holo-transferrin for its receptor being 800 times greater than that of apo-transferrin, we decided to work with the former, despite the relaxation induced on xenon by the paramagnetism of $Fe^{3+}$ ions. An alternative would have been, had the paramagnetic-induced relaxation reduced the NMR signal of hyperpolarized xenon too much, to replace iron atoms by gallium or indium atoms, which have similar affinities for TfR.[23]

In order to investigate the interaction of transferrin with its receptor in the presence of cells, two types of constructs were used.

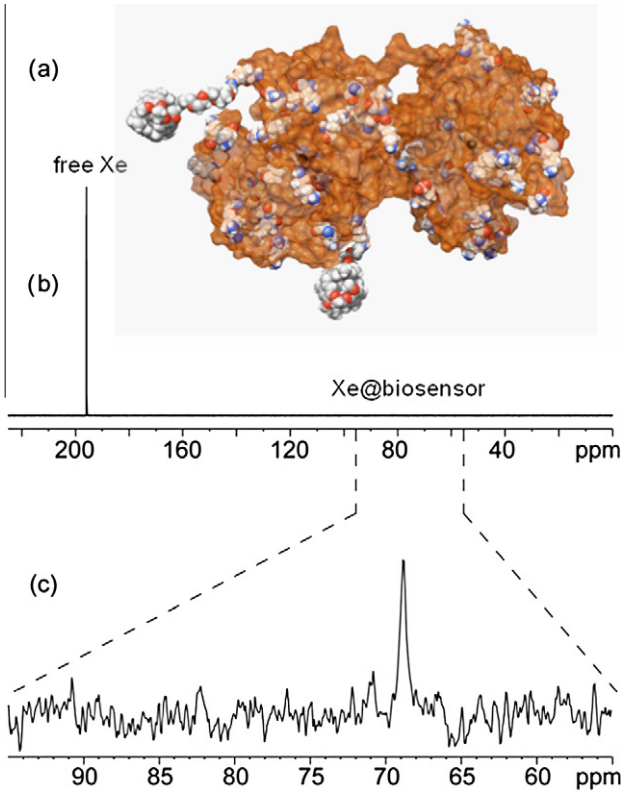


**Figure 2.** Example of a structure of the biosensors used and laser-polarized $^{129}$Xe NMR spectra of the noble gas dissolved in a 1.3 μM solution of **B1** in PBS (277 K, 11.7 T). On the construct displayed in (a), two cryptophane moieties are grafted on the protein. The lysine side chains are colored. Whereas the full spectrum in (b) was obtained in one scan with a hard pulse of small flip angle, the sub-spectrum in (c) was obtained by accumulation of 256 selective excitations with a repetition time of 122 ms. The 55–95 ppm frequency range, corresponding to the Xe@cryptophane region, is displayed.

In the first, a $^{129}$Xe NMR-based biosensor made with several cryptophanes per protein was built. As checked by $^1$H NMR, up to 10 cryptophanes could be grafted on transferrin before protein unfolding. A safe solution of five cryptophanes per protein was finally chosen and identified as biosensor **B1**. The second construct (biosensor **B2**) had a double modality: fluorescence and NMR. A statistical ratio of 2:2:1 was used for the cryptophane, fluorescent probe (rhodamine green) and protein, respectively. The fluorophore was grafted on the protein using the same strategy as for the cryptophane (see Section 4) and the folding of this protein construct **B2** was checked by $^1$H NMR. Finally, two other control constructs **B3** and **B4** were prepared. They corresponded to the previous biosensors except that bovine serum albumin (BSA) was used instead of transferrin. BSA has been widely used as a marker of fluid-phase pinocytosis.[24] Therefore, it is used to explore non-specific interaction with cell membranes. For the first biosensor,

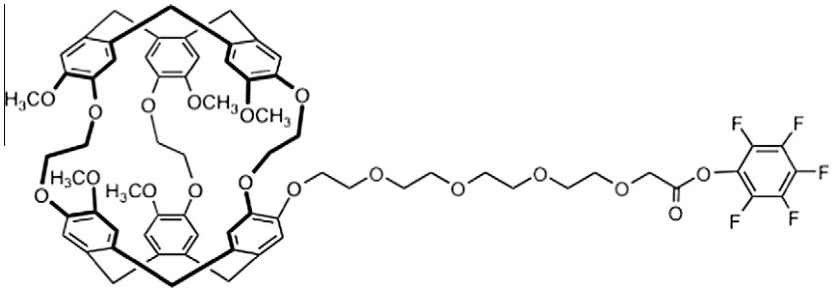


**Figure 1.** Chemical structure of the activated-ester cryptophane **1**.

the cryptophane precursor was grafted on BSA with a ratio of 5 cryptophanes per protein (biosensor **B3**). The second probe (the fluorescent biosensor **B4**) was built with a ratio of 2 cryptophanes and 2 rhodamine green moieties per BSA protein.

Figure 2 displays the $^{129}$Xe NMR spectra obtained at 11.7 T and 277 K with **B1** at 1.3 μM in PBS. Clearly the Xe@**B1** line is unique and not broad. This confirms that the spacer between the cryptophane part and the protein is long and flexible enough. From this experiment, the detection threshold using the direct observation method[5] has been estimated as 80 nM, or about 50 pmol using only 1 mL of gaseous hyperpolarized xenon. Obviously in the presence of the cells, the inherent loss of field homogeneity is likely to increase these limit values. For samples of apo- and holo-transferrin at 90 μM, $^{129}$Xe relaxation times of 450 ± 5 s and 147 ± 10 s have been measured, respectively. Therefore, at the concentration of biosensor used in the presence of cells (5 μM) relaxation due to paramagnetism does not represent a limitation.

### 2.2. Binding of the biosensors to K562 cells

The human erythroleukemic K562 cell line was chosen because it has a huge number of transferrin receptors on the plasma membrane: 1.6 $10^5$ receptors per cell (8 $10^5$ including the internalized receptors).[16,17] As our polarization level and our experimental protocol already enabled detection of $10^{12}$ xenon spins,[5] a rough calculation showed that $10^7$ cells in the detection volume should be enough.

It appeared difficult to envisage a direct MR contrast in a cell suspension, as our procedure includes shaking of the NMR tube to introduce fresh hyperpolarized xenon into solution. Furthermore, even if a tiny modification of the cryptophane environment is likely to give rise in the $^{129}$Xe NMR spectrum to a chemical shift variation of the Xe@biosensor signal when the biosensor is interacting with its biological target,[10] here for cell suspensions the line broadening due to susceptibility variation rendered such a detectable frequency separation unlikely. These difficulties led us to imagine the following 'batch' procedure, which is summarized in Figure 3. It is described here for biosensor **B1**, but strictly the same procedure was used for the other biosensors. In (a), 140 million K562 cells were incubated for one hour at 310 K with 3 mL of a solution of **B1** in PBS (final concentration 5 μM). After centrifugation at 277 K, the first supernatant gave rise to sample $s_a$ (supernatant *a*). After two further washings at 277 K, the cells were separated, giving rise to sample $c_a$ (cells *a*). In (b) in parallel, 140 million K562 cells were pretreated with pronase, a mixture of proteolytic enzymes that disable the function of TfR on the cell surface.[15,25] Following exactly the same procedure as in (a) we got samples $s_b$ and $c_b$, respectively.

The present protocol allowed pairwise comparison of the cell samples $c_a$ and $c_b$ through fluorescence microscopy when the biosensor **B2** was used, and through hyperpolarized $^{129}$Xe NMR with biosensor **B1**, as well as comparison between the supernatant samples $s_a$ and $s_b$.[26] As exchange of the transferrin biosensor between the intra- and extracellular compartments is driven by the laws of thermodynamics, this procedure was a way to 'freeze' the situation encountered during the incubation of the cells. Considering that the low temperature used for the washing steps and the conservation of the cells block the dynamics of the plasma membrane, this amounts to considering that the fluorescence images and $^{129}$Xe NMR spectra reflect the distribution of the biosensor at the end of the incubation step.

Figure 4 displays the fluorescence microscopy results. After incubation of the cells with **B2**, the internalization of the biosensor is clearly visible. The observation of clustered fluorescence inside the cells could be due to the presence of concentrated pools of **B2** within intracellular compartments. **B2** can also be found within the plasma membrane as indicated by the presence of green spots at the cell surface. After incubation of the K562 cells with pronase, no fluorescence was detected in the cell.

Figure 5 shows the 55–95 ppm chemical shift region of the laser-polarized $^{129}$Xe NMR spectra of both the cells incubated with **B1** and the supernatant samples. This chemical shift range exclusively corresponds to the signal of the noble gas encapsulated in the cryptophane.[5] In the $^{129}$Xe NMR spectrum of sample $c_a$, two peaks were observed in this region; in addition to the peak at 68–69 ppm, which was also observed in the isotropic solution (Fig. 2) or in the supernatant $s_a$ and corresponds to the biosensor in an aqueous environment, a second strong broad resonance at 79 ppm was observed. These two peaks had similar intensities. A quick calculation taking into account the number of cells present in solution and the estimated number of transferrin receptors per K562 cell revealed that the second peak cannot be assigned to xenon in the biosensor linked to the Tf receptor, whereas the first peak corresponds to the biosensor free in solution. For the current biosensor concentration, according to what is known for this biological system, the second peak should be much smaller. On the other hand, Meldrum et al. have shown that a chemical shift difference of up to 10 ppm can occur between xenon in the cryptophane

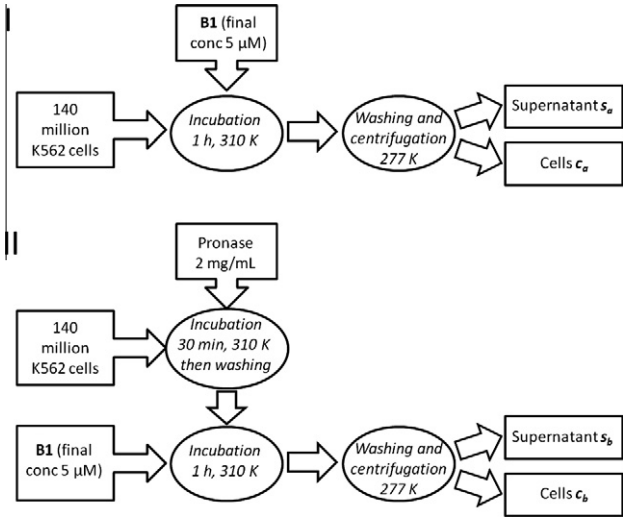


**Figure 3.** Synopsis of the batch experiments designed to study the interaction of the biosensor **B1** with the K562 cells.

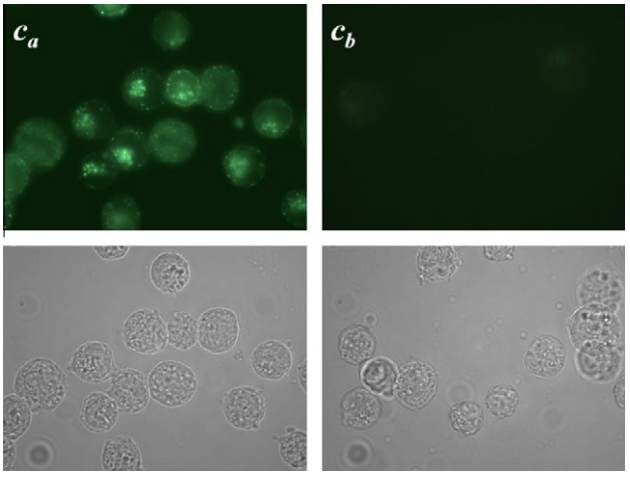


**Figure 4.** Fluorescence (up) and bright field (down) images of K562 cells incubated with the **B2** biosensor, without (left) and with (right) previous pronase treatment.

in the aqueous phase and xenon in the cryptophane in a lipid phase.[27] It thus seems more likely that the peak at 79 ppm can be assigned to the biosensor in the cell membrane. Whereas the left peak represents xenon encapsulated in his host located in the cell membrane, the peak at 69 ppm should contain the contribution of xenon in the intracellular aqueous compartment and in the free biosensor. Two facts substantiate this interpretation: (i) as endocytosis passes through the formation of endosomes, it could spread the biosensor—and therefore the cryptophane moiety—in either an aqueous or a membrane environment, even in the case of a selective interaction between the biosensor and the transferrin receptors; (ii) in a recent paper, we have shown that xenon crosses the cell membrane in some tens of milliseconds and keeps the major part of its hyperpolarization.[28]

As observed in Figure 5, only a very small and broad signal around 80 ppm was detected in the 55–95 ppm region of the $^{129}$Xe NMR spectrum of the $c_b$ sample, that is, the cells pre-incubated with pronase, although the xenon polarization level was close to that of the other cell sample $c_a$ (Table 1). This is in perfect agreement with the observations of fluorescence microscopy (Fig. 4). The resemblance between the xenon spectra of the supernatant samples ($s_a$ and $s_b$) ensures that the supernatant contains only the biosensor in aqueous environment.

A more quantitative examination of the relative area of the xenon peaks reveals many interesting features. The sum of the normalized peak areas for caged xenon in a series ($c_a + s_a$ or $c_b + s_b$) is nearly constant. This means that our biochemical procedure (incubation and washing steps) is robust, as the same amount of biosensor is recovered. This validates the fact that the absence of caged xenon signal in the sample $c_b$ results from biological changes in the sample and that the differences in peak integrals in this spectral region is indicative of the biological events.

In this batch experiment, the net difference between the $^{129}$Xe NMR spectra of the noble gas in the biosensor interacting with the cells after treatment or not by pronase (samples $c_b$ vs $c_a$) indicates that the transferrin receptors are required for a strong interaction of the biosensor with the cells.

**Table 1**
Peak areas extracted from the $^{129}$Xe NMR spectra of the different cell or supernatant samples

| Sample | $Xe_{free}$[a] | $Xe@B_{lipid}$[b] | $Xe@B_{water}$[c] | $Xe@B_{water}/Xe@B_{lipid}$ |
|---|---|---|---|---|
| $c_a$ | 4.68 | 169 | 100 | 0.59 |
| $s_a$ | 2.70 | 0 | 408 | — |
| $c_b$ | 1 | 9 | 0 | 0 |
| $s_b$ | 2.48 | 0 | 615 | — |
| $c_c$ | 2.94 | 157 | 44 | 0.28 |
| $s_c$ | 4.13 | 0 | 497 | — |

[a] The values given in this column are indicative of the xenon magnetization and can be compared.
[b] Corresponds to the signal at 79 ppm.
[c] Corresponds to the signal at 69 ppm. In each row the values of the second and third columns are normalized with respect to the value of the first column (and the value '100' was chosen for the peak of $Xe@B_{water}$ for $c_a$).

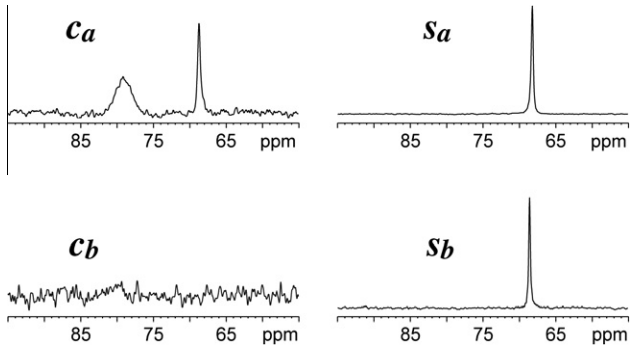


**Figure 5.** $^{129}$Xe NMR spectra obtained by selective excitation in the xenon@cryptophane spectral region (293 K; 11.7 T). Upper left: with K562 cells after incubation with the biosensor **B1** for 1 h at 310 K; upper right: spectrum of the corresponding supernatant; lower left: spectrum with K562 treated with pronase and then incubated with the biosensor **B1** for 1 h at 310 K; lower right: spectrum of the corresponding supernatant.

## 2.3. Further assessment of the specificity of the biosensor

Two other non-specific biosensors **B3** and **B4**, based on bovine serum albumin, were studied with K562 cells. The same procedure as before was followed, giving $c_c$ and $s_c$ samples. Figure 6 displays the fluorescence microscopy image obtained with biosensor **B4** and the laser-polarized $^{129}$Xe NMR spectrum of the $c_c$ sample. The fluorescence image is far less bright than that of the transferrin biosensor **B2**. In particular, unlike the case of **B2**, no bright internal spot can be observed inside the cells, a result in agreement with the absence of specific BSA receptor on the surface of the K562 cells enabling active internalization of the biosensor. In contrast, surprisingly two peaks appear again on the $^{129}$Xe NMR spectrum of **B3** with K562 cells, tending to indicate an interaction between BSA and the K562 cells. Again, the sum of the normalized integrals ($c_c + s_c$) is comparable to ($c_a + s_a$) or ($c_b + s_b$), thus validating our procedure.

To explain the propensity of **B3** as well as of **B1** to interact non-specifically with the cells we could assume that the hydrophobicity of the cryptophane moieties anchors both biosensors in the cell membrane. To address this point, another experiment was performed. Two new transferrin-based constructs were built. In the first, the fluorescent probe was grafted (again via the lysine side chains) on apo-transferrin (two rhodamine green moieties per protein). In the second, the fluorescent probe and the cryptophane precursor were grafted on apo-transferrin, at a ratio 2:2 for one protein. These constructs were introduced in solutions containing giant unilamellar vesicles. Comparison of the bright field and fluorescence microscopy images obtained in both cases is displayed in Figure S1 of the Supplementary data. A strong difference was observed between the two images. Whereas the fluorescence was rather diffuse in the case of the rhodamine green-labeled protein (no interaction is expected with the vesicles), the location of the second construct in the vesicle lipid bilayer was clearly visible. This interaction must be due to the presence of the cryptophane moieties on the second construct, proving that the hydrophobic character of the cage-molecule is likely to induce non-specific interaction with the cells via their membrane.

Even if these non-specific interactions prevent straightforward analysis of the NMR results, various observations indicate that a real biosensor has been prepared. The ratio between the caged xenon peaks is more in favor of the cryptophane in the aqueous part for **B1** than for **B3** (0.59 vs 0.28, see Table 1). Logically the normalized areas of xenon in the biosensors in a lipid environment are similar for **B1** and **B3**, as the same number of cells of the same line is expected to offer the same number of membrane sites. The presence of a $^{129}$Xe NMR signal corresponding to **B3** in the cells may be explained by the non-specific internalization of the probe by pinocytosis.[24] This hypothesis is in agreement with the diffuse inner fluorescent signal observed in Figure 6.

Pairwise comparison of the sums of the peak areas in the $^{129}$Xe NMR spectra for the biosensors in the presence of cells ($c_a$ vs $c_c$) reveals that 33% more signal is present for **B1** than for **B3**. This confirms that the specific interaction of **B1** with its receptors induces endocytosis, preventing the release of the biosensor at the washing step. This observation proves that the biosensor is recognized by the K562 cells, even if it is also subjected to nonspecific interaction

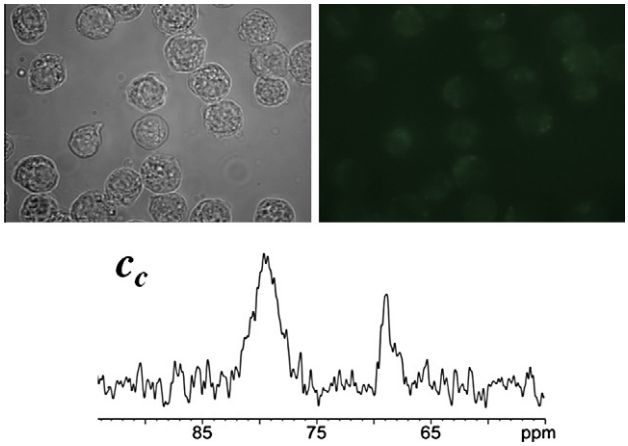


**Figure 6.** Bright field (left) and fluorescence (right) images of K562 cells incubated with the **B4** biosensor, and $^{129}$Xe NMR spectrum of K562 cells incubated with the **B3** biosensor, obtained by selective excitation in the xenon@cryptophane spectral region (293 K; 11.7 T).

with the cells due to the hydrophobic character of the cryptophane moieties.

## 3. Conclusion

In this article, a new strategy for the building of efficient $^{129}$Xe NMR biosensors is developed. It is based on the nonspecific grafting of cryptophane precursors on the primary amines of a protein interacting with a specific receptor. This gives versatility to the approach and enables further gain in sensitivity by the multiplicity of xenon hosts on the protein.

This method has been applied to the transferrin system in vitro. Study through hyperpolarized $^{129}$Xe NMR of the biosensor interacting with K562 cells reveals several features. Firstly, even for an unmodified biological system containing a high level of paramagnetism, NMR of hyperpolarized species in stable and reproducible experiments is possible. At the concentrations of protein used (~5 μM), the observed xenon relaxation time remains long, which enables full use to be made of the reservoir of polarization constituted by dissolved xenon. Moreover, given the large reservoir of gaseous hyperpolarized xenon on top of the solution, if required we can use additional spectra to increase the signal-to-noise ratio simply by shaking the NMR tube between two acquisition series.

Secondly, fluorescence microscopy experiments prove that the biosensor is recognized by the Tf receptors of the K562 cells and endocytosed despite the presence of the cryptophane and fluorophore moieties at the surface of the protein. The large differences between hyperpolarized $^{129}$Xe NMR spectra of the biosensor alone, of the biosensor in the presence of cells, intact and pre-treated with pronase, confirm this result. For the first time, a specific $^{129}$Xe spectral signature is observed and correlated to a biological process. Thanks to an original methodology leading to a quantitative analysis, this biological interaction mediated by the transferrin receptors is validated.

An additional experiment using a BSA biosensor has however pointed out the presence of nonspecific interaction contributing to the signal. It seems reasonable thinking that it results from the strong hydrophobic character of the cryptophane. Without leading to protein unfolding, it tends to attract the biosensor to the cell membrane. This shows that the current approaches aimed at solubilizing cryptophanes in water by introducing a hydrophilic ligand far from the cavity can have some drawbacks, as already observed with a cryptophane biosensor designed to recognize a complementary DNA strand in solution.[10] The amphiphilicity created by the presence of the cage-molecule and the aliphatic spacer on one side and the oligonucleotide on the other side led to the formation of self-organized systems of the micelle or vesicle type. A solution will be to place hydrophilic groups closer to the aromatic rings of the cryptophanes, while ensuring maintenance of the xenon in–out exchange.[29]

This in vitro study demonstrates the feasibility of detecting a biological mechanism using hyperpolarized $^{129}$Xe NMR-based biosensors in the presence of live cells and paves the way for the conception of an improved biosensor addressing water solubility, bio-distribution and toxicity issues that will be determinant for the success of this approach in vivo.

## 4. Experimental

### 4.1. General

All the solvents were distilled before use (DMF from calcium hydride under reduced pressure, acetone and $CH_2Cl_2$ from calcium chloride, THF from benzophenone ketyl). Column chromatographic separations were carried out over Merck silica gel 60 (0.040–0.063 mm). Analytical thin-layer chromatography (TLC) was performed on Merck silica gel TLC plates F254. Mass spectra were recorded in LSIMS mode on a ThermoFinnigan MAT95XL spectrometer. Exact mass measurements were obtained by 'peak matching'. $^1$H and $^{13}$C NMR spectra were recorded on Bruker Avance 500 spectrometers. Chemical shift $\delta$ ($^1$H, $^{13}$C) are given relative to $Me_4Si$.

### 4.2. Synthesis of the cryptophane moieties

Derivative **1** was prepared using cryptophane-A (**2**) and a PEG chain (**3**) as starting materials.

#### 4.2.1. Synthesis of cryptophanol-A 4 (Scheme 1)

Cryptophanol **4** (whose synthesis has been independently reported by Darzac et al.[30,31] and Spence et al.[9]) was prepared in a single step from cryptophane-A **2**. Removal of a single methyl group of **2** was easily achieved by using iodotrimethylsilane in $CH_2Cl_2$ at room temperature. This synthetic route yielded cryptophanol in 37% yield as well as unreacted cryptophane-A, which could be reused for subsequent reactions:

Pure iodotrimethylsilane (65 μL, 0.455 mmol) was added in one portion using a syringe to a stirred solution of cryptophane-A **2** (400 mg, 0.45 mmol) in $CH_2Cl_2$ (8 mL). The solution was stirred in the dark for 16 h under an argon atmosphere at room temperature. $CH_2Cl_2$ (10 mL) was added and the solution was acidified with 1 M HCl (6 mL). The organic layer was collected, washed with water and then dried over sodium sulfate. After evaporating the solvent under reduced pressure the residue was purified on a column chromatography ($CH_2Cl_2$/$Et_2O$: 90/10) to give the cryptophanol **4** as a white solid (144 mg, 37%). Spectroscopic data are identical to those previously reported for this compound.[30]

#### 4.2.2. Synthesis of the linker (Scheme 1)

The PEG linker used for the attachment of the biosensor molecule to the protein was prepared in three steps from the mono-protected PEG **3**, whose synthesis has been reported previously.[32–34] An activated acid function was then introduced at one extremity in order to allow coupling with the protein and a tosyl group at the other extremity to allow coupling with cryptophanol **4**.

**4.2.2.1. 3,6,9,12-Tetraoxatetradecanoic acid,14-[[tetrahydro-2*H*-pyran-2-yl]oxy]phenylmethyl ester (5).** 2-[2-[2-[2-[(tetrahydro-2*H*-pyran-2-yl)oxy]ethoxy]ethoxy]-ethoxy]ethanol (5 g, 18 mmol, 1 equiv) in THF (60 mL) was added dropwise to a stirred solution of NaH 60% (1.8 g, 45 mmol, 2.5 equiv) in THF (50 mL) under an argon atmosphere. After complete addition the mixture was

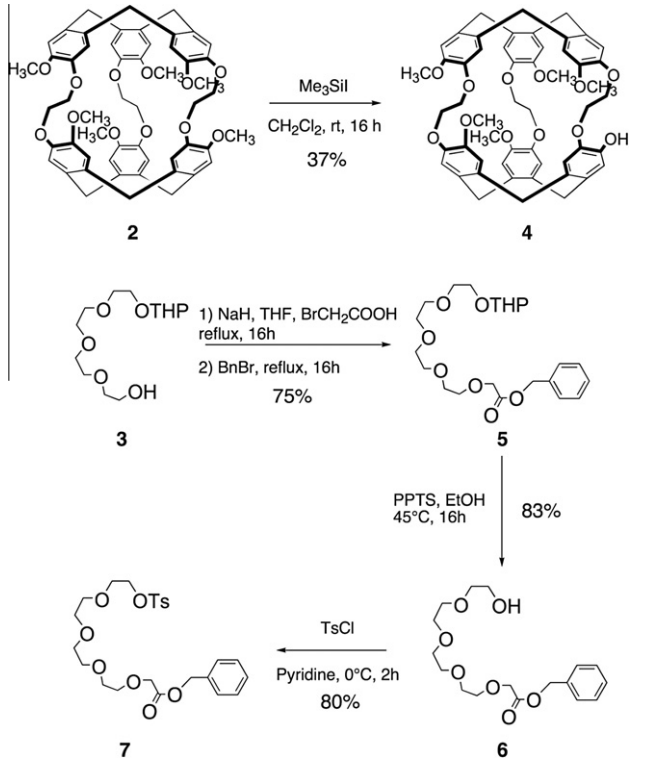


**Scheme 1.** Synthesis of cryptophanol-A (**4**) and synthesis of the linker (**7**).

stirred for an additional 1 h. A solution of bromoacetic acid (2.8 g, 20 mmol, 1.1 equiv) in THF was then added dropwise. After addition the solution was heated overnight under reflux conditions. The solution was allowed to reach room temperature and benzyl bromide (2.3 mL, 19.3 mmol, 1.1 equiv) was added in one portion. The solution was then heated overnight under reflux conditions. After evaporating the solvent under reduced pressure, $CH_2Cl_2$ (250 mL) and water (100 mL) were added. The layers were separated and the aqueous layer was extracted twice with $CH_2Cl_2$ (100 mL). The combined organic layers were then washed twice with water (50 mL) and dried over sodium sulfate. After evaporation of the solvent the crude product was purified by column chromatography (AcOEt) to give **5** as a colorless oil (5.75 g, 75%). $^1$H NMR (500 MHz, $CDCl_3$, 298 K) $\delta$ 7.35–7.28 (m, 5H; Ar), 5.15 (s, 2H; $OCH_2Bn$), 4.59 (m, 1H, OCHO), 4.17 (s, 2H, $OCH_2COO$), 3.85–3.80 (m, 2H; $OCH_2$), 3.71–3.69 (m, 2H, $OCH_2$), 3.66–3.60 (m, 12H, $OCH_2$), 3.59–3.54 (m, 1H, $OCH_2$), 3.48–3.44 (m, 1H, $CH_2$), 1.82–1.76 (m, 1H, $CH_2$), 1.71–1.65 (m, 1H; $CH_2$), 1.60–1.44 (m, 4H; $CH_2$). $^{13}$C NMR (125.7 MHz, $CDCl_3$, 298 K) $\delta$ 170.26, 135.38, 128.53, 128.35, 128.33, 98.85, 70.88, 70.57, 70.55, 70.53, 70.50, 70.46, 68.61, 66.57, 66.41, 62.12, 30.49, 25.36, 19.41. HRMS $[M+Na]^+$. Calcd 449.2117. Found 449.2142.

**4.2.2.2. 3,6,9,12-Tetraoxatetradecanoic acid-14-hydroxyphenylmethyl ester (6).** A stirred solution of **5** (4.98 g, 11.3 mmol, 1 equiv) and pyridinium toluene sulfonate (0.95 g, 3.78 mmol, 0.33 equiv) in ethanol was heated overnight at 318 K. The solvent was removed under reduced pressure and the oily residue purified by column chromatography (AcOEt). Evaporation of the solvent gave **6** as a colorless oil (3.2 g; 83%). Spectroscopic data are identical to those previously reported in the literature.[35]

**4.2.2.3. 3,6,9,12-Tetraoxatetradecanoic acid-14-[[(4-methylphenyl)sulfonyl]oxy]-phenylmethyl ester (7).** Para-chloro toluene sulfonate (1.5 g, 7.87 mmol, 1.3 equiv) was added at 273 K in one portion to a stirred solution of 6 (2 g, 5.84 mmol) in pyridine (6 mL). The solution was stirred at this temperature for an additional 2 h. Water (10 mL) and diethyl ether (40 mL) were then added to the solution. The organic layer was collected and the aqueous layer was extracted twice with diethyl ether ($2 \times 20$ mL). The combined organic layers were washed with brine (20 mL) and water (10 mL) and dried over sodium sulfate. Evaporation of the solvent leaves a residue, which was purified by column chromatography (AcOEt). Different fractions were collected and the evaporation of the solvent gave **7** (2.32 g, 80%) as a colorless oil. Spectroscopic data are identical to those previously reported in the literature.[36] Additional information $^1$H NMR (500 MHz, $CDCl_3$, 298 K) $\delta$ 7.77 (d, 3J(H,H) = 8.3 Hz, 2H; Ar), 7.33–7.29 (m, 7H; Ar), 5.16 (s, 2H; $OCH_2Bn$), 4.17 (s, 2H; $OCH_2COO$), 4.13 (t, 3J(H,H) = 4.9 Hz, 2H; $OCH_2$), 3.71–3.54 (m, 14H, $OCH_2$), 2.42 (s, 3H; $CH_3$).

### 4.2.3. Synthesis of cryptophane 1 (Scheme 2)

The coupling reaction between cryptophanol **4** and PEG **7** was carried out in DMF in the presence of cesium carbonate. The reaction gave rise to the monofunctionalized cryptophane **8** in 69% yield. The deprotection of the carboxylic acid was then achieved by hydrogenation under atmospheric pressure in the presence of a Pd/C catalyst in $CH_2Cl_2$/EtOH solution to give **9** in 89% yield. Finally, the carboxylic acid group was activated by introducing a pentafluorophenol moiety in the presence of 1-(3-dimethylaminopropyl)-3-ethylcarbodiimide hydrochloride in $CH_2Cl_2$. to give the desired cryptophane **1**.

**4.2.3.1. Synthesis of cryptophane 8.** 3,6,9,12-Tetraoxatetradecanoic acid-14-[[(4-methylphenyl) sulfonyl]oxy]phenylmethyl ester (**7**) (254 mg, 0.51 mmol, 1.5 equiv) was introduced in a three-neck flask containing cesium carbonate (167 mg, 0.51 mmol), cryptophanol **4** (300 mg, 0.34 mmol) in freshly distilled DMF (12 mL). The mixture was stirred for 16 h under argon atmosphere at 333 K. $CH_2Cl_2$ (25 mL) and brine (10 mL) were added to the mixture. The aqueous layer was extracted twice with $CH_2Cl_2$ (10 mL) and the combined organic layers were washed with brine ($5 \times 10$ mL) and then dried over sodium sulfate. The solvent was removed under reduced pressure to give a residue, which was then purified on silica gel (a gradient of solvent $Et_2O$/AcOEt was used: 100/0; 80/20; 50/50; 0/100). Evaporation of the solvent gave compound **8** as a white amorphous solid (282 mg, 69%). $^1$H NMR (500 MHz, $CDCl_3$, 298 K) $\delta$ 7.33–7.32 (m, 5H, Ar), 6.77 (s, 1H; Ar), 6.74 (s, 1H; Ar), 6.73 (s, 1H; Ar), 6.72 (s, 1H; Ar); 6.71 (s, 2H; Ar), 6.67 (s, 1H; Ar); 6.66 (s, 1H; Ar), 6.65 (s, 2H; Ar), 6.64 (s, 1H; Ar), 5.16 (s, 2H; $OCH_2Bn$), 4.59–4.53 (m, 6H; Ha), 4.19–.10 (m, 15H, $OCH_2$, $OCH_2COO$); 3.93 (m, 1H); 3.80–3.66 (m, 30 H; $OCH_2$ and $OCH_3$), 3.39–3.35 (m, 6H; He). $^{13}$C NMR (125.7 MHz, $CDCl_3$, 298 K) $\delta$ 170.32, 162.50, 149.85, 149.73, 149.61, 149.56, 148.96, 147.20, 146.72, 146.67, 146.62, 146.59, 135.45, 134.31, 134.26, 134.12, 134.04, 133.99, 132.72, 131.83, 131.57, 131.54, 131.47, 131.36, 128.60, 128.42, 128.39, 122.30, 121.39, 121.26, 120.54, 120.47, 120.33, 117.03, 114.64, 113.70, 113.59, 70.94, 70.86, 70.75, 70.65, 69.88, 69.60, 69.53, 69.38, 69.29, 69.20, 68.73, 68.64, 68.48, 56.09, 55.73, 55.66, 55.64, 55.59, 36.46, 36.30. HRMS $[M+Na]^+$. Calcd 1227.4949. Found 1227.4935.

**4.2.3.2. Synthesis of cryptophane 9.** $H_2$ gas was introduced into a 25 mL flask containing compound **8** (560 mg, 0.465 mmol), $CH_2Cl_2$ (12 mL), ethanol (2 mL), and Pd/C (70 mg, 0.0658 mmol, 0.14 equiv). The mixture was stirred at room temperature for 5 h. After completion of the reaction the mixture was filtered and the solid residue was washed with $CH_2Cl_2$ ($2 \times 10$ mL). The solvent was then removed under reduced pressure to give the carboxylic acid derivative **9** (0.46 g; 89%). $^1$H NMR (500 MHz, $CDCl_3$, 298 K) $\delta$ 6.77 (s, 1H; Ar), 6.74 (s, 1H; Ar), 6.73 (s, 3H; Ar), 6.725 (s, 1H;

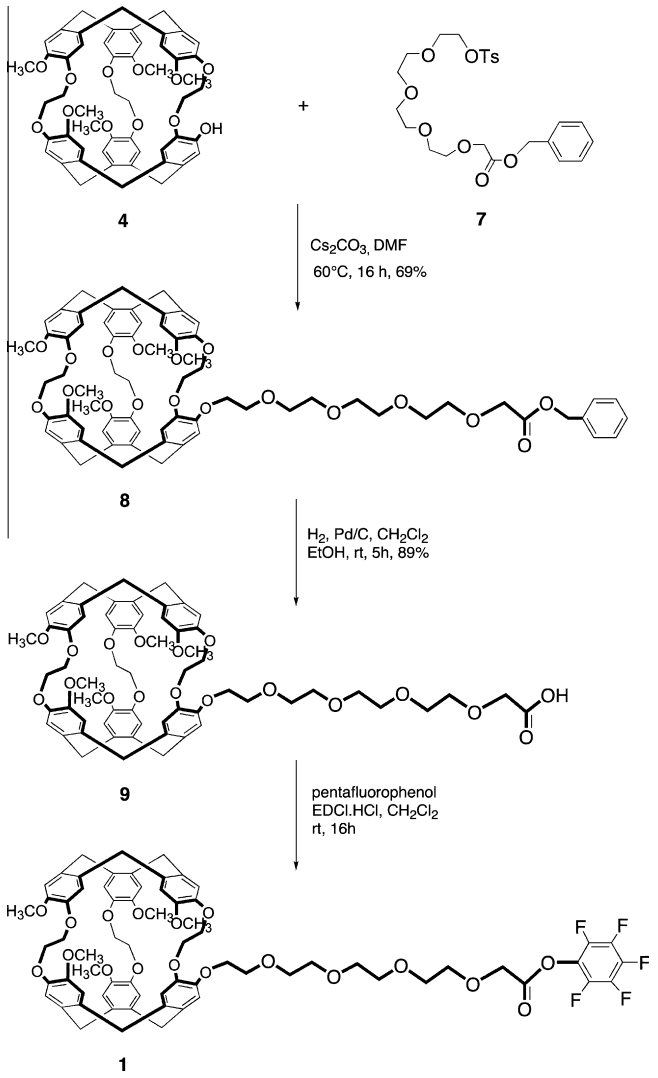


**Scheme 2.** Synthesis of the activated cryptophane **1** from cryptophanol **4**.

Ar), 6.72 (s, 2H; Ar), 6.69 (s, 1H; Ar), 6.66 (s, 1H; Ar), 6.65 (s, 3H; Ar); 4.59–4.53 (m, 6H; Ha); 4.21–4.12 (m, 15H; $OCH_2$ and $OCH_2$-COO), 3.95 (m, 1H), 3.82 (t, 2H, 3 J(H,H) = 5.0 Hz), 3.78–3.73 (m, 27 H, $OCH_2$–$OCH_3$), 3.41–3.36 (m, 6H, He). $^{13}C$ NMR (125.7 MHz, $CDCl_3$, 298 K) $\delta$ 170.99, 149.83, 149.71, 149.63, 149.59, 149.55, 148.91, 147.21, 146.65, 146.60, 134.39, 134.26, 134.16, 134.09, 134.00, 132.75, 131.87, 131.59, 131.54, 131.40, 122.17, 121.28, 120.59, 120.54, 120.38, 117.12, 114.72, 113.72, 113.61, 71.59, 70.88, 70.76, 70.64, 70.37, 70.18, 69.85, 69.59, 69.53, 69.38, 69.31, 69.23, 69.13, 69.72, 56.16, 55.74, 55.66, 55.64, 55.60, 36.22, 36.20, 36.15. HRMS $[M+Na]^+$. Calcd 1137.4460. Found 1137.4452.

**4.2.3.3. Cryptophane 1: activation of the carboxylic acid function of 9.** Cryptophane **9** (76 mg, 0.068 mmol, 1 equiv) pentafluorophenol (0.019 g, 0.1 mmol; 1.5 equiv) and $CH_2Cl_2$ (0.5 mL) were introduced into a 10 mL three-neck flask. The mixture was stirred for 15 min at room temperature and then 1-(3-dimethylaminopropyl)-3-ethylcarbodiimide (13 mg, 0.068 mmol; 1 equiv) was added in one portion. The reaction mixture was stirred overnight at room temperature. $CH_2Cl_2$ (5 mL) and a saturated solution of $NaHCO_3$ (2 mL) were then added to the reaction mixture. The two layers were separated and the organic layer was washed with brine and then dried over sodium sulfate. Evaporation of the solvent under reduced pressure leaves a residue, which was purified by preparative TLC (AcOEt/$Et_2O$: 70/30). From this procedure 3 mg of the desired cryptophane moiety **1** was isolated and used without further treatment for the coupling reaction with the protein.

### 4.3. Preparation of the biosensors

The human transferrin and BSA were from Sigma–Aldrich. Rhodamine green succinimide ester was from Molecular Probes.

#### 4.3.1. Grafting of cryptophane

The proteins were incubated with the activated cryptophane for 1 h in phosphate buffered saline (PBS) pH 7.4 at room temperature with stirring. The unreacted cryptophane was finally removed from the protein solution using Sephadex G25 medium gel chromatography. The elution was performed with PBS, pH 7.4.

#### 4.3.2. Grafting of Rhodamine green

The proteins were incubated with the fluorescent dye in bicarbonate medium pH 8.4 for 1 h, at room temperature with stirring. The unreacted dye was removed from the protein solution using Sephadex G25 medium gel chromatography. The elution was performed with PBS, pH 7.4. Labeling efficiency was checked using an absorption spectrometer.

#### 4.3.3. Construction of the various biosensors

**B1** was obtained after the incubation of 5 molecules of cryptophane per molecule of transferrin; **B2**, after the incubation of two molecules of cryptophane and two molecules of rhodamine green per molecule of transferrin; **B3**, after the incubation of five molecules of cryptophane per molecule of BSA; **B4**, after the incubation of two molecules of cryptophane and 2 molecules of rhodamine green per molecule of BSA.

### 4.4. Characterization of the constructs

The folding of the biosensors was checked by NMR on a 700 MHz Bruker spectrometer equipped with an HCN cryoprobe. Solutions at 1 mM in 500 µL $H_2O$:$D_2O$ 90:10 were analyzed in 5 mm tubes. The presence of high field $^1H$ resonances and the chemical shift dispersion of the amide and aromatic $^1H$ resonances were used as an indicator of the preservation of the global fold of the protein. A maximum of ten cryptophanes could be tethered to transferrin. Beyond this value, the protein unfolds. A statistical distribution of the number of cryptophanes and of their locations on the protein was expected; however mass spectrometry data indicated a narrow distribution of the number of grafted cryptophanes. In addition, $^1H$ translational self-diffusion experiments were performed on a 500 MHz Avance II Bruker spectrometer equipped with a TBI HN-broadband probehead and a BGU II gradient unit. These diffusion experiments at different concentrations were performed to confirm that cryptophanes were covalently linked and not trapped inside anfractuosities of the protein.

### 4.5. Cells

#### 4.5.1. Cell culture

Human erythroleukemic K562 cells from ATCC were grown in IMDM medium (Sigma–Aldrich) supplemented with 10% heat-inactivated fetal bovine serum, 1% of L-glutamine, 100 U/ml penicillin and 100 g/ml streptomycin. The cells were maintained in exponential growth in a 5% $CO_2$ incubator at 310 K. Prior to the experiment, the cells were washed three times in PBS and viable cells were counted using the trypan blue exclusion test. The chosen number of cells was re-suspended to a final volume of 1.5 mL.

#### 4.5.2. Fluorescent labeling

Cells were incubated with 200 nM of fluorescent probe for 1 h. The cells were washed 3 times with PBS at 277 K to block the membrane dynamics. The cells were then were fixed on the glass substrate using 5% PFA for 30 min at 277 K. The observation was made using an inverted microscope.

#### 4.5.3. Preparation of the pronase sample

The cells were treated with a 2 mg/mL solution of pronase for 30 min at 310 K. The cells were then re-washed three times with PBS and incubated with 5 μM of the biosensor for 1 h at 310 K. Finally, the cells were washed three times at 277 K to block plasma membrane dynamics, and re-suspended in a final volume of 1.5 mL. Their viability was checked through the trypan blue exclusion test.

### 4.6. $^{129}$Xe NMR experiments

#### 4.6.1. Laser-polarized xenon

Xenon 86%-enriched in isotope 129 was from Cortecnet, France. The hyperpolarized gas was prepared by the spin-exchange method, using our batch apparatus described previously.[37,5] The amount of gas produced with this set-up using a titanium:sapphire laser, on the order of 1 mL (in ~10 minutes), was sufficient to fill the NMR tube with a pressure of ~1 bar and an average polarization of 40%. The transfer of xenon between the cold finger designed to separate xenon from nitrogen after optical pumping and the NMR tube of interest was made through a vacuum line in the fringe field of the NMR magnet in order to preserve polarization.

#### 4.6.2. $^{129}$Xe hyperpolarized NMR experiments

The experiments were run on a 500 MHz Avance II Bruker spectrometer equipped with a $^{129}$Xe/$^{1}$H micro-imaging probehead (Micro-5) designed for tubes with a maximum outer diameter of 8 mm. Prior to the NMR experiments, the samples inside the NMR tubes were degassed by the following procedure: helium bubbling then static evacuation of the gas on top of the solutions in a vacuum line. Each series of acquisitions was preceded by shaking (to quickly dissolve the hyperpolarized gas) and a wait time of ~10 s to enable the elimination of bubbles.

For each experiment, that is, for each cell or supernatant sample, exactly the same procedure was employed: after the shaking of the tube, a first $^{129}$Xe spectrum acquired with non-selective pulse of small flip angle (~4°) was recorded in one scan. This was immediately followed by three series of sub-spectra obtained by selective excitation centered on the Xe@cryptophane region, then detection.[5] The selective excitation was performed using a 1% truncated Gaussian pulse of 500 μs. Three series of 128 scans differing by the repetition time (70 ms, 100 ms, 170 ms) allowed us to eliminate the potentially different xenon in-out exchange rates. This set of four experiments could be repeated many times after shaking of the tube as long as the reservoir of gaseous xenon gave significant polarization to the dissolved xenon.

The spectra were processed as follows: a line broadening of 20 Hz (no zero-filling) was applied before Fourier transformation. As exactly the same conditions (same receiver gain, in particular) were used for the non-selective spectra, the integration values can be directly compared (first column of Table 1). Except for the repetition time, the sub-spectra were also acquired in the same experimental conditions, but obviously here the receiver gain was different from that of the non-selective experiments. Within each series the three sub-spectra were summed, and the peak integral values were divided by the integral value of the peak in the corresponding non-selective experiment, in order to eliminate the polarization fluctuations. So the values of the second and third columns can be directly compared. Due to the high xenon magnetization available in the gaseous phase, the values given in Table 1 correspond to the sum of two non-selective spectra for the first column, and six selective sub-spectra (two tube shakings) for the second and third columns.

## Acknowledgments

Support from the French Ministry of Research (project ANR-06-PCVI-0023 BULPOXI) is acknowledged.

## Supplementary data

Supplementary data associated with this article can be found, in the online version, at doi:10.1016/j.bmc.2011.05.002.

## References and notes

1. Walker, T. G.; Happer, W. *Rev. Mod. Phys.* **1997**, *69*, 629.
2. Comment, A.; Jannin, S.; Hyacinthe, J.-N.; Miéville, P.; Sarkar, R.; Ahuja, P.; Vasos, P. R.; Montet, X.; Lazeyras, F.; Vallée, J.-P.; Hautle, P.; Konter, J. A.; van den Brandt, B.; Ansermet, J.-Ph.; Gruetter, R.; Bodenhausen, G. *Phys. Rev. Lett.* **2010**, *105*, 018104.
3. Brunner, E. *Concepts Magn. Reson.* **1999**, *11*, 313.
4. Spence, M. M.; Rubin, S. M.; Dimitrov, I. E.; Ruiz, E. J.; Wemmer, D. E.; Pines, A.; Qin Yao, S.; Tian, F.; Schultz, P. G. *Proc. Natl. Acad. Sci. U.S.A.* **2001**, *98*, 10654.
5. Berthault, P.; Huber, G.; Desvaux, H. *Prog. NMR Spectrosc.* **2009**, *55*, 35.
6. Brotin, T.; Dutasta, J.-P. *Chem. Rev.* **2009**, *109*, 88.
7. Lerouge, F.; Melnyk, O.; Durand, J.-O.; Raehm, L.; Berthault, P.; Huber, G.; Desvaux, H.; Constantinesco, A.; Choquet, P.; Detour, J.; Smaïhi, M. *J. Mater. Chem.* **2009**, *19*, 379.
8. Berthault, P.; Bogaert-Buchmann, A.; Desvaux, H.; Huber, G.; Boulard, Y. *J. Am. Chem. Soc.* **2008**, *130*, 16456.
9. Spence, M. M.; Ruiz, E. J.; Rubin, S. M.; Lowery, T. J.; Winssinger, N.; Schultz, P. G.; Wemmer, D. E.; Pines, A. *J. Am. Chem. Soc.* **2004**, *126*, 15287.
10. Roy, V.; Brotin, T.; Dutasta, J.-P.; Charles, M.-H.; Delair, T.; Mallet, F.; Huber, G.; Desvaux, H.; Boulard, Y.; Berthault, P. *ChemPhysChem* **2007**, *8*, 2082.
11. Wei, Q.; Seward, G. K.; Hill, P. A.; Patton, B.; Dimitrov, I. E.; Kuzma, N. N.; Dmochowski, I. J. *J. Am. Chem. Soc.* **2006**, *128*, 13274.
12. Chambers, J. M.; Hill, P. A.; Aaron, J. A.; Han, Z.; Christianson, D. W.; Kuzma, N. N.; Dmochowski, I. J. *J. Am. Chem. Soc.* **2009**, *131*, 563.
13. Schlundt, A.; Kilian, W.; Beyermann, M.; Sticht, J.; Günther, S.; Höpner, S.; Falk, K.; Roetzschke, O.; Mitschang, L.; Freund, C. *Angew. Chem., Int. Ed.* **2009**, *48*, 4142.
14. Seward, G. K.; Wei, Q.; Dmochowski, I. J. *Bioconjug. Chem.* **2008**, *19*, 2129.
15. Du, X.-L.; Wang, K.; Ke, Y.; Yuan, L.; Li, R.-C.; Chang, Y. Z.; Ho, K. P.; Qian, Z. M. *J. Cell. Physiol.* **2004**, *201*, 45.
16. Klausner, R. D.; Ashwell, G.; van Renswoude, J.; Harford, J. B.; Bridges, K. R. *Proc. Natl. Acad. Sci. U.S.A.* **1983**, *80*, 2263.
17. Klausner, R. D.; van Renswoude, J.; Ashwell, G.; Kempf, C.; Schechter, A. N.; Dean, A.; Bridges, K. R. *J. Biol. Chem.* **1983**, *258*, 4715.
18. Lowery, T. J.; Garcia, S.; Chavez, L.; Ruiz, E. J.; Wu, T.; Brotin, T.; Dutasta, J.-P.; King, D. S.; Schultz, P. G.; Pines, A.; Wemmer, D. E. *ChemBioChem* **2006**, *7*, 65.
19. The chirality of the resulting molecules arises from the chirality of the cryptophane (see Ref. 6). As the grafting of the PEG group was made on a racemic mixture of cryptophanes, the risk was to obtain two signals for caged xenon. Putting the first asymmetric carbon far from the cavity where xenon will reside, promises a non-significant chemical shift variation for xenon caged in both diastereomers.
20. Partis, M. D.; Griffiths, D. G.; Roberts, G. C.; Beechey, R. B. *J. Protein Chem.* **1983**, *2*, 263.
21. Wang, W.; Ackermann, D.; Mehlich, A.-M.; König, S. *Proteomics* **2010**, *10*, 1525.
22. Kida, S.; Maeda, M.; Hojo, K.; Eto, Y.; Nakagawa, S.; Kawasaki, K. *Chem. Pharm. Bull.* **2007**, *55*, 685.
23. Sun, H.; Li, H.; Sadler, P. J. *Chem. Rev.* **1999**, *99*, 2817.
24. Pinaud, F.; Clarke, S.; Sittner, A.; Dahan, M. *Nature. Meth.* **2010**, *7*, 275.
25. Qian, Z. M.; Morgan, E. H. *Biochim. Biophys. Acta* **1991**, *1073*, 456.
26. Despite a xenon polarization level not fully reproducible, quantitative estimation of the xenon NMR signals has been rendered possible through normalization of the integral of the peak of xenon free in solution, considering that the same amount of xenon was each time introduced in the NMR tube (checked by weighting of the tube before and after the experiment).
27. Meldrum, T.; Schröder, L.; Denger, P.; Wemmer, D. E.; Pines, A. *J. Magn. Reson.* **2010**, *205*, 242.
28. Boutin, C.; Desvaux, H.; Carrière, M.; Leteurtre, F.; Jamin, N.; Boulard, Y.; Berthault, P. accepted in NMR Biomed. doi:10.1002/nbm.1686.
29. Berthault, P.; Desvaux, H.; Wendlinger, T.; Gyejacquot, M.; Stopin, A.; Brotin, T.; Dutasta, J.-P.; Boulard, Y. *Chem. Eur. J.* **2010**, *16*, 12941.
30. Darzac, M.; Brotin, T.; Bouchu, D.; Dutasta, J.-P. *Chem. Commun.* **2002**, 48.

31. Darzac, M.; Brotin, T.; Rousset-Arzel, L.; Bouchu, D.; Dutasta, J.-P. *New J. Chem.* **2004**, *28*, 502.
32. Sakellariou, E. G.; Montalban, A. G.; Beall, S. L.; Henderson, D.; Meunier, H. G.; Phillips, D.; Suhling, K.; Barrett, A. G. M.; Hoffman, B. M. *Tetrahedron* **2003**, *59*, 9083.
33. Barluenga, J.; de Prado, A.; Santamaría, J.; Tomás, M. *Organometallics* **2005**, *24*, 3614.
34. Kaufmann, G. F.; Mejler, M. M.; Sun, C. Z.; Chen, D. W.; Kujawa, D. P.; Mee, J. M.; Hoffman, T. Z.; Wirsching, P.; Lerner, R. A.; Janda, K. D. *Angew. Chem., Int. Ed.* **2005**, *44*, 2144.
35. Marchi-Artzner, V.; Lorz, B.; Hellerer, U.; Kantlehner, M.; Kessler, H.; Sackmann, E. *Chem. Eur. J.* **2001**, *7*, 1095.
36. Marchi-Artzner, V.; Jullien, L.; Gulik-Krzywicki, T.; Lehn, J.-M. *Chem. Commun.* **1997**, 117.
37. Desvaux, H.; Gautier, T.; Le Goff, G.; Pétro, M.; Berthault, P. *Eur. Phys. J. D* **2000**, *12*, 289.